Iran. J. Radiat. Res., 2009; 6 (4): 173-182

Determination of the optimum filter for qualitative and quantitative ^{99m}Tc myocardial SPECT imaging

M. N. Salihin Yusoff[1*] and A. Zakaria[1,2]

[1] School of Health Science, University Science Malaysia, Kelantan, Malaysia
[2] Department of Nuclear Medicine, Radiotherapy and Oncology, University Science Malaysia Hospital, Kelantan, Malaysia

Background: Butterworth, Gaussian, Hamming, Hanning, and Parzen are commonly used SPECT filters during filtered back-projection (FBP) reconstruction, which greatly affect the quality and size accuracy of image. ***Materials and Methods:*** This study involved a cardiac phantom in which 1.10 cm thick cold defect was inserted into its myocardium wall and filled with 4.0 μCi/ml (0.148 MBq/ml) ^{99m}Tc concentration. The cardiac insert was then put into a cylindrical tank which was filled with 1.2 μCi/ml (0.044 MBq/ml) ^{99m}Tc concentration as background. 272 combinations of filter parameters were selected from those filters and applied on image. The measurements of count in myocardium, background, and defect regions of interest (ROI) were performed on each filtered image. Those measurements were then used to calculate contrast, signal-to-noise ratio (SNR), and defect size. For every filter, each criterion was graded (1 to 100) and then summed at their specific setting for total comparison. ***Results:*** The results show that, the different filter types produced myocardial image with different contrast, SNR, and defect size. For contrast and SNR, Gaussian filter was the best, while Parzen filter was the best in producing accurate defect size. However, Butterworth filter was found the best for trade off between contrast, SNR, and defect size accuracy. ***Conclusion:*** Selection of filter should consider the type of analysis, whether qualitatively or quantitatively. Qualitative analysis depends on image quality which is denoted by high contrast and SNR, thus Gaussian filter was suggested. Instead, the Butterworth filter was suggested for quantitative analysis as it is greatly dependent on both, image quality and size accuracy.
Iran. J. Radiat. Res., 2009; 6 (4): 173-182

Keywords: *^{99m}Tc myocardial SPECT, image filtering.*

INTRODUCTION

Filtered back-projection (FBP) is the widely used method for SPECT image reconstruction. In clinical practice, filter is used during reconstruction to reduce image noise, increase contrast and signal-to-noise ratio (SNR), and enhance the ability to detect any abnormalities. In principle, filter is a mathematical function that is applied to pixels in an image. The goal of filtering is to eliminate as much noise and retain as much signal as possible [(1)]. This includes smoothing, edge enhancement, and resolution recovery. Most of filters are characterized by cut off frequency and order parameters. The cut off frequency defines the frequency from which higher frequencies will be suppressed and therefore denotes the bandwidth of the filter. The amplitude of the filter at cut off frequency is dependent on the type of the filter. Some filters such as Butterworth and Gaussian are defined by a second parameter, the order of the filter. This parameter tunes the filter by changing the slope of the filter function and allows the user to optimise the trade off smoothness–sharpness of the image [(2)].

The choosing of filter and its parameters depend on several factors [(2)]. First, it depends on the number of counts (limited by patient radiation burden and by movement artefacts related to study time). Second, it depends on the organ of study. The different organs have different amount of radiotracer administered, thus need to a different filter parameters [(3)].

**Corresponding author:*
Muhammad Nur Salihin Yusoff, Medical Radiation Programme, School of Health Science, University Science Malaysia, 16150 Kubang Kerian, Kelantan, Malaysia.
E-mail: *mnsalihin@gmail.com*

[Downloaded from ijrr.com on 2024-03-28]

Third, it depends on the background of noise level. If the background of noise level is too low and the contrast is already sufficient for clinical evaluation, filtering is not necessary. Fourth, it depends on the choice of interpretation. It is because the optimal filter parameters for qualitative or visual analysis may be quite different from optimal filter parameters for quantification [4, 5].

However, there is no standard filter for universal application in clinical studies and only very limited literature exists on selection of appropriate filter parameters for practical purposes [2, 6]. The choosing of the appropriate filter, cut off frequency and order is a matter of trial and error and ought to be the function of the specific radioisotope, protocol, and imaging system used [7, 8]. Inappropriate filtering of the raw back-projected tomographic data may significantly degrade image quality and affect the accuracy of quantitative results [6, 9 –11]. So, this study was carried out so that the effect of SPECT filters on myocardial image quality could be compared, thus determined the optimum filter for visual and quantitative analyses.

SPECT Filters

Ramp

The ramp filter is a high pass filter used in SPECT imaging. Its mathematical function is shown in equation 1.

$$H_R(k_x, k_y) = k = \sqrt{k_x^2 + k_y^2} \qquad (1)$$

Ramp filter is always used during FBP reconstruction to reduce the 1/r blurring or star artifact [2]. Ramp filter enhance high frequency noise in the image, which is associated with low counting statistics. In practice, ramp filter is not used alone but with combination of additional filter (low pass filter) to reduce the enhancement of high frequency noise.

Butterworth

The Butterworth filter is one of the most popular low pass filters used in SPECT imaging especially in nuclear cardiology [12]. It is because the ability to change its shape through the cut off frequency and order parameter which allows better adaptation of the filter function to the frequency characteristics of the projection data [1]. Butterworth filter in spatial frequency domain (f) has two parameters; the cut off frequency (f_c), and the order of the filter (n) (equation 2) [12].

$$B(f) = \frac{1}{1 + \left(\frac{f}{f_c}\right)^{2n}} \qquad (2)$$

Gaussian

The Gaussian filter is a band pass spatial frequency filter which has two variables; the displacement from the origin (f_c) and the spread (n) as described in equation 3. The equation is one-dimension of Gaussian filter function, which (f) is spatial frequency [13].

$$G(f) = e^{\frac{-(f-f_c)^2}{2n^2}} \quad u \geq 0 \qquad (3)$$

Hamming

The Hamming filter is one of low pass filter used to remove high frequency noise in SPECT imaging. It is simpler than Butterworth filter, having only a single parameter to describe its shape, referred to as the cut off frequency [14]. This filter is defined in frequency domain as shown in equation 4, where (f_c) is cut off frequency and (f) is spatial frequency.

$$H(f) = \begin{cases} 0.54 + 0.46\cos\left(\frac{\pi f}{f_c}\right) & 0 \leq |f| \leq f_c \\ 0 & otherwise \end{cases} \qquad (4)$$

Hanning

The Hanning filter is also a low pass filter which has only a single parameter to describe its shape; that is the cut off frequency [14]. Its filter function is quite

[Downloaded from ijrr.com on 2024-03-28]

similar to Hamming filter as shown in equation 5, where (f_c) is cut off frequency and (f) is spatial frequency [15]. The difference of Hanning to Hamming filters is only on the amplitude at the cut off frequency, which the amplitude of Hanning filter at that point is going to zero.

$$H(f)=\begin{cases}0.50+0.50\cos\left(\dfrac{\pi f}{f_c}\right) & 0\le|f|\le f_c\\ 0 & otherwise\end{cases} \quad (5)$$

Parzen

The Parzen filter is a smoothing filter which it application can result a low resolution and low noise level in an image [2]. This filter is obtained by piecing together two fourth-degree polynomials separately defined in two subintervals of the frequency range $(0,f_c)$ as shown in equation 6 [16].

$$P(f)=\begin{cases}|f|-6|f|\left(\dfrac{|f|}{f_c}\right)^2\times\left(1-\dfrac{|f|}{f_c}\right) & \left(|f|<\dfrac{f_c}{2}\right)\\ 2|f|\left(1-\dfrac{|f|}{f_c}\right)^3 & \left(\dfrac{f_c}{2}<|f|<f_c\right)\\ 0 & \left(|f|\ge f_c\right)\end{cases} \quad (6)$$

MATERIALS AND METHODS

Preparing Phantom

Myocardial wall chamber (250 ml) with 1.1 cm thick cold defect made of plastic at the anterior (figure 1) was filled with water and 1000 µCi (37 MBq) of ^{99m}Tc, yielded a ^{99m}Tc concentration of about 4.0 µCi/ml (0.148 MBq/ml). The cardiac phantom was then placed into the cylindrical tank (10 litres) and its position was adjusted to mimic human heart relative to the gamma camera. The cylindrical tank was then filled with water and 1200 µCi (44.4 MBq) of ^{99m}Tc, yielding a ^{99m}Tc concentration of about 1.2 µCi/ml (0.044 MBq/ml) as background.

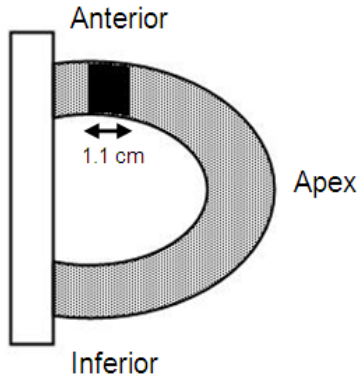


Figure 1. The plastic rod (cold defect) was located at the anterior position of cardiac insert (viewed from vertical axis).

Data Acquisition

Data acquisition was obtained with dual head, large field of view gamma camera (ADAC Forte Imaging System), equipped with low energy high resolution (LEHR) collimators. 64 projections (25 sec per projections) was taken in 64 x 64 matrix (pixel size was 6.47 mm) using step and shoot acquisition over 180° arc from 45° right anterior oblique (RAO) to 45° left posterior oblique (LPO) position, with radius of 29.7 cm. The distance between detectors and phantom was approximately 2 cm. A single energy window at 140 keV was used.

Calculation of Background-Target Counts Ratio

The background-target counts ratio (BTR) was calculated from raw image using Lung-Heart Ratio program. Two regions of interest (ROI) were defined over the cardiac zone and a representative background region of an anterior or left anterior oblique (LAO) 45° projection image. Then, the program automatically calculated the counts ratio.

Data Processing

Data processing was performed using AutoSPECT program. SPECT slices were

[Downloaded from ijrr.com on 2024-03-28]

reconstructed from raw image using filtered back-projection (FBP) with ramp filter. In AutoSPECT ramp filter is automatically utilized in reconstruction process. Five filters with 272 combinations of filter parameters were combined with ramp filter as follow: Butterworth (cut off: 0.20-0.80 Nq with step 0.05, order: 3-12 with step 1), Gaussian (cut off: 0.20-0.80 Nq with step 0.05, order: 10-22 with step 2), Hamming (cut off: 0.20-1.00 Nq with step 0.05), Hanning (cut off: 0.20-1.00 Nq with step 0.05), Parzen (cut off: 0.20-1.00 Nq with step 0.05). The SPECT slices obtained were then reoriented into three standard views, which were along short axis, vertical long axis and horizontal long axis.

Calculation of Contrast, Signal-to-Noise Ratio, and Defect Size

There were 272 SPECT slices were selected for calculations. For each slice, a line was drawn on vertical long axis view of phantom image at defined region of interest (ROI) to measure the maximum count in normal myocardium ($R_{max\ (myo)}$), minimum count in defect ($R_{min\ (def)}$), and minimum count in background (heart hole region) ($R_{min\ (hole)}$). To determine the defect size, a line was drawn on the defect. Two peaks of different count (because of different attenuation) were observed. The number of pixel between the smaller peak and the steep of the other peak having same count (N_{pixel}) was measured. All of these measurements were performed using Count Profile program (figure 2). Then, by using all of these measurements, the maximum contrast, signal-to-noise ratio (SNR), and size of defect were calculated according to these formulas:

$$Max\ \ Contrast\ \ , C = \frac{R_{\max\ (myo)} - R_{\min\ (def)}}{R_{\max\ (myo)}} \quad (7)$$

$$SNR\ \ , S = \frac{R_{\max\ (myo)} - R_{\min\ (def)}}{R_{\min\ (hole)}} \quad (8)$$

$$Defect\ \ Size\ , D = N_{pixel} \times 6.47\ mm \quad (9)$$

where 6.47 mm is a pixel size.

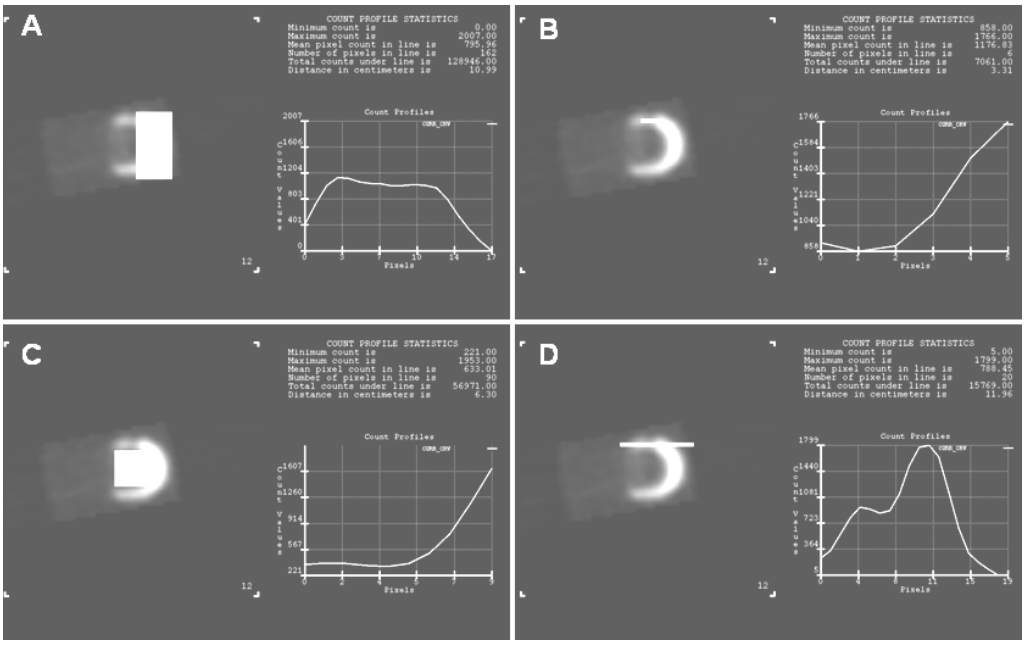


Figure 2. The measurements of maximum count in normal myocardium ($R_{max\ (myo)}$) (A), minimum count in defect ($R_{min\ (def)}$) (B), minimum count in background or heart hole region ($R_{min\ (hole)}$) (C), and number of pixel between the smaller peak and the steep of the other peak having same count (N_{pixel}) (D) using Count Profile program.

[Downloaded from ijrr.com on 2024-03-28]

Analysis of Data

The determination of the optimum filter for qualitative (visual) myocardial SPECT would consider the ability of each filter type in producing high contrast and SNR. Therefore, the contrast and SNR for every filter were analyzed. However, there are many contrast and SNR values in every filter type due to the different combination of filter parameters used. To analyze the whole ability of that filter (in producing contrast and SNR), the mean contrast and mean SNR were calculated. The filter which has the highest mean contrast and SNR was chosen as the optimum filter for qualitative analysis.

While, the determination of the optimum filter for quantitative myocardial SPECT would consider the ability of each filter types in producing high contrast, SNR, and defect size accuracy. Therefore, the total grade (trades off between contrast, SNR, and defect size) was analyzed. To calculate total grade, the grading method used by Takavar *et al.*, (2004) was applied [17]. For every filter, each parameter (contrast, SNR, and defect size) were first graded from 1 to 100; 1 for worst and 100 for the best contrast and SNR, while 1 for the longest and 100 for the nearest defect size to the true size (1.10 cm). For the sake of simplicity in grading process, the SPECT slices having defect size below the true size were excluded.

RESULTS

Raw Image and SPECT Slices

Figure 3 shows the raw image of cardiac phantom and SPECT slices in short-axis, vertical long-axis, and horizontal long-axis views. Average total counts are approximately 20.5 million which is about 320 kcounts per projection. The calculated background-target counts ratio is 0.60. In the short-axis and vertical long-axis views, a defect can be observed at the anterior of myocardial wall chamber.

Contrast

Table 1 summarizes the contrast for five filters calculated from 272 SPECT slices with different combination of filter parameters. The Gaussian shows the highest maximum contrast, that is 0.82. The plotted mean contrast shows Gaussian is the best filter for contrast, that is 0.64 ± 0.08 (figure 4A).

Signal-to-Noise Ratio

Table 2 summarizes the SNR for five filters. The SNR range for Gaussian filter is very large compared to others, which the maximum is 1038.00. The plotted mean SNR shows Gaussian is the best filter for SNR, that is 58.28 ± 172.73 (figure 4B).

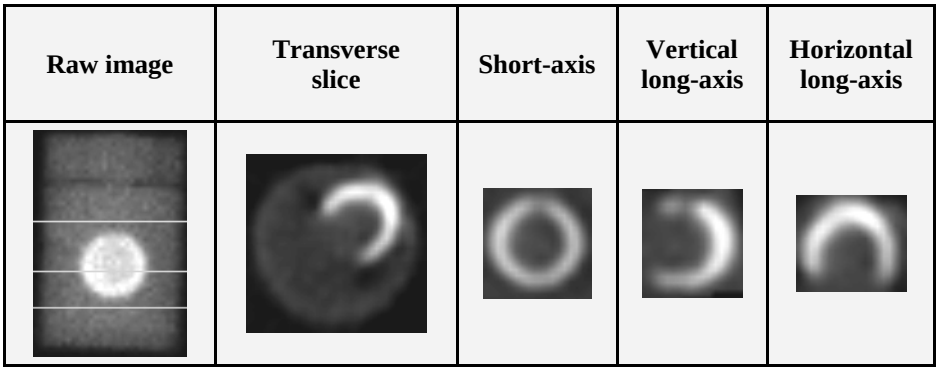


Figure 3. The raw image and SPECT slices in three standard views. The defect could be observed visually, located at the anterior position in short-axis and vertical long-axis images.

[Downloaded from ijrr.com on 2024-03-28]

Defect Size

Table 3 summarizes the defect size for five filters. The maximum defect size for Butterworth and Gaussian filters are approximately double of its true size (1.10 cm), those are 2.04 cm and 2.82 cm respectively. Parzen filter shows the smallest changes, which its mean values is the nearest defect size to the true size (1.27 ± 0.08 cm) (figure 4C).

Total Grade

Table 4 summarizes the total grade for five filters. The maximum total grade for Gaussian filter is the highest (75.94), however its mean value is the lowest (35.25 ± 7.93). The maximum total grade for Hamming, Hanning, and Parzen are same (67.00). The Butterworth filter has the highest mean total grade, that is 55.59 ± 9.23 (figure 4D).

Table 1. Summary of contrast for five filters.

Filter	Contrast			
	Minimum	Maximum	Mean	Std. Deviation
Butterworth	0.53	0.62	0.60	0.02
Gaussian	0.53	0.82	0.64	0.08
Hamming	0.51	0.54	0.52	0.01
Hanning	0.51	0.53	0.52	0.01
Parzen	0.50	0.51	0.50	0.00

Table 2. Summary of SNR for five filters.

Filter	SNR			
	Minimum	Maximum	Mean	Std. Deviation
Butterworth	2.33	3.27	2.99	0.21
Gaussian	2.57	1,038.00	58.28	172.73
Hamming	2.09	2.33	2.22	0.09
Hanning	2.11	2.29	2.20	0.08
Parzen	1.84	1.91	1.88	0.03

Table 3. Summary of defect size for five filters.

Filter	Defect Size (cm)			
	Minimum	Maximum	Mean	Std. Deviation
Butterworth	1.17	2.04	1.86	0.23
Gaussian	1.24	2.82	1.88	0.37
Hamming	1.20	1.51	1.37	0.12
Hanning	1.17	1.47	1.33	0.12
Parzen	1.16	1.35	1.27	0.08

Table 4. Summary of total grade for five filters.

Filter	Total Grade (1 to 100)			
	Minimum	Maximum	Mean	Std. Deviation
Butterworth	26.67	68.20	55.59	9.23
Gaussian	29.16	75.94	35.25	7.93
Hamming	34.00	67.00	50.23	14.49
Hanning	34.00	67.00	49.95	15.92
Parzen	28.13	67.00	47.70	18.27

[Downloaded from ijrr.com on 2024-03-28]

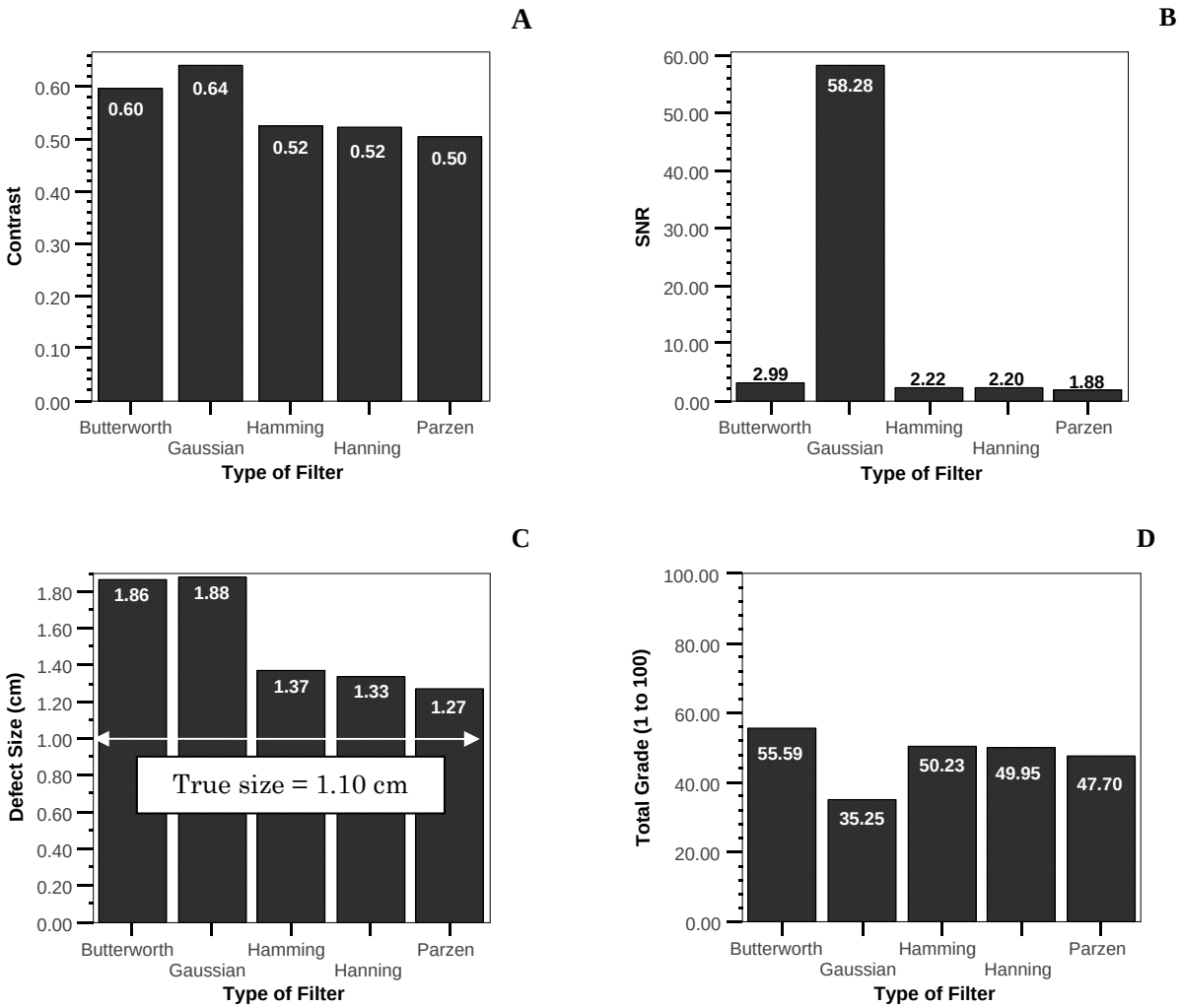


Figure 4. Comparison of mean contrast (A), SNR (B), defect size (C), and total grade (D) among the five filters.

DISCUSSION

The raw image in this study has sufficient total counts based on the fact that a total of 6 million counts were required to reconstruct tomographic images with statistical noise (assuming for an object occupies 75 % of total image area in a 64 × 64 matrix typically used in SPECT) [18]. The calculated background-target counts ratio is analogous to the lung-heart ratio (LHR), a quantitative parameter in describing myocardial uptake relative to the lung. This study shows that the background-target counts ratio is 0.60. According to Germano (2006), the preliminary data for ^{99m}Tc suggests an upper limit of normal is 0.44 [19].

All filters used in this study are passive filters, which the Butterworth, Hamming, Hanning, and Parzen filters are low pass filters (which allows low frequencies pass), while the Gaussian is band pass filter (which allow certain range of frequencies pass) [13,16]. However, in FBP reconstruction with ramp filter, the combined low pass filters also function as a band pass filter.

Different mathematical functions of those filters affect the image quality

[Downloaded from ijrr.com on 2024-03-28]

differently especially for Butterworth and Gaussian filters. While the effect of Hamming, Hanning, and Parzen on image quality are quite similar. There are disagreement between high contrast and SNR, and accurate defect size. For qualitative analysis, the weighing down should be on contrast and SNR, while the size precision is important for quantitative analysis. The high contrast and SNR are also needed in quantitative analysis as it can facilitate the detection process by algorithms.

The Gaussian filter shows the best in producing image with high contrast and SNR, however it is worst in producing accurate defect size. In this study, the defect size for Gaussian filter can increase more than double of its true size. This is risky for quantitative analysis of myocardial SPECT as it tends to give false results. The total grade of Gaussian filter is interesting to be analyzed, which their maximum shows the highest among the five filters, but their mean value is the worst. It means that several of Gaussian filter parameters are appropriate for usage. A further study should be performed to determine the cut off frequency and order for Gaussian filter which produces the best contrast and SNR.

The Butterworth filter is moderate for all parameters among the five filters. Although the mean contrast, SNR, and defect size of Butterworth filter are not the best, but its mean total grade shows the highest. It means that the Butterworth filter has the ability to balance between the needs of high contrast, SNR, and accurate size. This ability is important especially for quantification, which is greatly dependent on the image quality and size precision. Usually, the quantifications are performed automatically by computer using specific algorithms. This is an advantage of Butterworth filter, making it the most popular SPECT filter used in myocardial SPECT imaging [12].

CONCLUSION

It is important to choose the right filter during FBP reconstruction. We suggest the Gaussian filter to be used for visual analysis of myocardial SPECT because of its ability to produce the high quality image. Instead, the Butterworth filter is suggested for quantitative analysis because of its ability to balance between image quality and size accuracy.

ACKNOWLEDGEMENT

This study is supported by Ministry of Science, Technology, and Innovation (MOSTI) Malaysia under postgraduate scheme.

REFERENCES

1. Groch MW, Erwin WD (2000) SPECT in the year 2000: basic principles. *J Nucl Med Technol,* ***28****: 233-244.*
2. Laere KV, Koole M, Lemahieu L, Dierckx R (2001) Image filtering in single-photon emission computed tomography: principles and applications. *Comput Med Imaging Graph*, ***25****: 127-133.*
3. Ohnishi H, Ota T, Takada M, Kida T, Noma K, Matsuo S, Masuda K, Yamamoto I, Morita R (1997) Two optimal prefilter cutoff frequencies needed for SPECT images of myocardial perfusion in a one-day protocol. *J Nucl Med Technol*, ***25****: 256-260.*
4. Minoshima S, Maruno H, Yui N, Togawa T, Kinoshita F, Kubota M, Berger KL, Uchida Y, Uno K, Arimizu N (1993) Optimization of Butterworth filter for brain SPECT imaging. *Ann Nuc Med,* ***7****: 71-79.*
5. Wheat JM, Currie GM (2007) A Comparison of strategies for summing gated myocardial perfusion SPECT: are false negatives a potential problem? *Internet J Cardiol,* ***4****.*
6. Manrique A, Hitzel A, Gardin I, Dacher JN, Vera P (2003) Impact of Wiener filter in determining the left ventricular

[Downloaded from ijrr.com on 2024-03-28]

volume and ejection fraction using Thallium-201 gated SPECT. *Nucl Med Commun,* ***24****: 907-914.*

7. Germano G, Nichols KJ, Cullom SJ, Faber TL, Cooke CD (2001) Gated perfusion SPECT: technical considerations. In: *Cardiac SPECT imaging*, (DePuey EG, Garcia EV, Berman DS, eds.), Lippincott Williams & Wilkins, USA.
8. Mann A (2004) Quality control for myocardial perfusion imaging. In: *Nuclear cardiology, practical applications*, (Heller GV, Hendel RC, eds.), The MacGraw Hill Companies Inc, USA.
9. Vera P, Manrique A, Pontvianne V, Hitzel A, Koning R, Cribier A (1999) Thallium-gated SPECT in patients with major myocardial infarction: effect of filtering and zooming in comparison with equilibrium radionuclide imaging and left ventriculography. *J Nucl Med,* ***40****: 513-521.*
10. Wright GA, McDade M, Martin W, Hutton I (2002) Quantitative gated SPECT: the effect of reconstruction filter on calculated left ventricular ejection fractions and volumes. *Phys Med Biol,* ***47****: N99-N105.*
11. Vakhtangandze T, Hall DO, Zananiri FV, Rees MR (2005) The effect of Butterworth and Metz reconstruction filters on volume and ejection fraction calculations with Tc-99m gated myocardial SPECT. *Brit J Radiol,* ***78****: 733-736.*
12. Germano G (2001) Technical aspect of myocardial SPECT imaging. *J Nucl Med,* ***42****: 1499-1507*.
13. Madsen MT, Park CH (1985) Enhancement of SPECT images by fourier filtering the projection image set. *J Nucl Med,* ***26****: 395-402*.
14. Cullom SJ (2001) Principles of cardiac SPECT. In: *Cardiac SPECT imaging,* (DePuey EG, Garcia EV, Berman DS, eds.), Lippincott Williams & Wilkins, USA.
15. Gilland DR, Tsui BMW, McCartney WH, Perry JR, Berg J (1988) Determination of the optimum filter function for SPECT imaging. *J Nucl Med,* ***29****: 643-650.*
16. Rusinek H (1995) SPECT reconstruction techniques. In: *Clinical SPECT imaging,* (Kramer EL, Sanger JJ, eds.), Raven Press. Ltd, New York, USA.
17. Takavar A, Shamsipour G, Sohrabi M, Eftekhari M (2004) Determination of optimum filter in myocardial SPECT: a phantom study. *Iran J Radiat Res,* ***1****: 205-210.*
18. Zanzonico P (1995) Technical requirements for SPECT: instrumentation, data acquisition and processing, and quality control. In: *Clinical SPECT imaging,* (Kramer EL, Sanger JJ, eds.), Raven Press. Ltd, New York, USA.
19. Germano G (2006) Quantitative analysis in myocardial SPECT imaging. In: *Quantitative analysis in nuclear medicine imaging,* (Zaidi H, eds.), Springer Science & Business Media, USA.

[Downloaded from ijrr.com on 2024-03-28]

[Downloaded from ijrr.com on 2024-03-28]